# Thermal Instability Analysis of a Synchronous Generator Rotor using Direct Mapping

**A. Narain Singh*, W. Doorsamy** and W. A. Cronje ***

** University of the Witwatersrand, 1 Jan Smuts Avenue, Braamfontein 2000 Johannesburg, South Africa. Email: amesh.singh@eskom.co.za, Willie.Cronje@wits.ac.za*
*** University of Johannesburg, PO Box 17011, Doornfontein, 2028, Johannesburg, South Africa. Email:za.wesley.doorsamy@ieee.org*

**Abstract:** This paper presents a direct and practical method for mapping the thermal behaviour of a synchronous generator. Since temperature variations can lead to rotor thermal instability which adversely affects the operation of the generating unit, a better understanding of this phenomenon is required. The two main methods of performing thermal instability testing - direct current injection and friction/windage - are found to be practiced internationally without preference. Infrared thermography is used here as a means of determining the thermal performance of the rotor under different testing scenarios. The experimental testing is conducted using a scaled setup of a balancing facility and a 600 MW generator rotor. The results obtained are presented in the form of surface temperature maps. The thermal distribution of the two different methods were found to differ substantially with the friction method exhibiting a uniform surface distribution while the current method exhibited areas of higher temperature concentration around the rotor pole faces.

**Key words:** Infrared thermography, synchronous generator, thermal instability testing.

## 1. INTRODUCTION

Thermally induced imbalances of a generator rotor experienced during operation can lead to excessive mechanical vibration that far exceeds the operating limits of the rotor. The result of which can be a tripped unit with a loss of generating capacity or a generator operating with a load loss – to maintain stability. Furthermore, this creates a rather difficult fault finding process to identify and correct the root cause of the thermally induced vibration. This condition is commonly referred to as rotor thermal instability. Thermal Instability Testing (TIT) is common practice for major utilities and is performed at specially designed balancing facilities or in situ to determine the thermal behaviour of rotors. TIT is generally performed after any major refurbishment work which has been conducted on the rotor i.e. rewind, slot liner replacements, major overhaul, retaining ring replacement etc. [1]. Two main testing methods are used worldwide: 1) Direct current injection into the rotor winding and, 2) Windage or friction heating. Different utilities prefer specific tests based on their own propriety experiences. The variations in methodology and lack of published data supporting either of the aforementioned tests create uncertainty as to which test is able to best detect any latent thermal imbalances within the rotor assembly.

This paper presents a method for mapping the thermal distribution of a generator rotor under different test conditions. The direct thermal mapping of the rotor body is presented using a down-scaled model of a 600 MW generator rotor. This method utilises a practical approach - as opposed to any simulations - to determine the thermal behaviour of the rotor. A simulation approach requires modelling of all the physical details of the rotor. It is both impractical and computationally expensive to capture such a complex construction to a level of detail suitable for TIT. This practical approach is beneficial as it provides a physical measurement to determine the exact thermal distribution of the rotor and ascertain its behaviour under different conditions. This will assist in determining which tests are better suited to detecting rotor thermal instability.

## 2. ROTOR THERMAL INSTABILITY

In essence, thermal instability occurs when a change in the field current causes a corresponding change in vibration levels. A rotor that is both mechanically and electrically balanced – is deemed stable and fit for service. Conversely – if a rotor is unbalanced – the resulting uneven loading will lead to bowing of the rotor shaft and increased vibration levels.

Thermally induced vibrations may be the result of one or a combination of the following:

- Shorted Turns - One of the most common failure mechanisms on a generator rotor is inter-turn shorts. Shorted turns occur when there is a breakdown in the insulation between turns. These shorted turns can cause thermal and/or magnetic imbalances. This can be accompanied by mechanical vibration as well.
- Coil movement - During the heating cycle coils may move to one side of the rotor creating a ratcheting effect that leads to imbalance.
- Blocked ventilation slots or inadequate cooling - Restrictions in cooling can severely affect the thermal balance of the rotor. This results in an uneven temperature distribution along the length of the rotor generating an imbalance.

- Non-uniform winding - If the rotor is not wound uniformly from pole to pole with the same insulation thickness and build up materials, differences in frictional forces may result leading to a restriction in expansion of the copper coils.
- Blocking - Blocking used within the overhangs of the rotor must be spaced and fitted correctly to ensure uniform expansion of the coils without restriction. Incorrectly fitted blocking can result in coil restriction and the rotor bowing.
- Body wedges - Ill-fitting rotor body wedges that may be too loose or too tight create an uneven interference fit throughout the slot length. This can lead to the restriction of movement of copper coils in the axial direction resulting in a thermal bend.
- Tight Slots - Rewound rotors may sometimes experience tight slots when the original copper is being reused. The original copper may not be symmetrical and flat after years of usage. Design clearances are then compromised creating an uneven expansion within the slots causing thermal bowing of the rotor [1- 4].

## 3. OVERVIEW OF TIT METHODS

Three methods of performing TIT on large turbo-generator rotors are practiced. The first is an online test performed in-situ after the rotor has been commissioned. The remaining two tests are conducted at a balancing facility that is capable of either performing a Friction Thermal Instability Test (FTIT) or a Current Thermal Instability Test (CTIT). In general, facilities that can perform a CTIT can also perform a FTIT but not vice versa. It should be noted that no international standard exists with testing methodologies or acceptance criteria for vibration limits when performing TIT.

### *3.1 Windage/Friction TIT (FTIT)*

Reference material regarding FTIT is scarce; the method however is prominent within the power industry. Local utility experience regarding this test involves the rotor being operated at rated speed where the frictional (windage) interaction between the rotor surface and surrounding air causes the rotor to heat. Rapid or controlled heating is not possible when using this method. Vibration and temperature values are monitored throughout the test and it can be performed at any balancing facility as no specialised equipment is required. The convenience of the FTIT is one of the main reasons for it being so popular in practice.

### *3.2 Current Excitation TIT (CTIT)*

CTIT is a specialised test which requires a balancing facility that is capable of injecting current into the rotor and also equipped to deal with the resulting electrical field. The details of this test methodology are not well published. In [5], some information regarding this type of test, as performed by an OEM, is given however the actual procedure is described as a patented solution. Essentially, the level of current injected into the rotor at rated speed is gradually increased. The test comprises of three phases - i.e. heating phase, stabilisation phase and final cooling phase. The temperature of the rotor and vibration of both the pedestal and shaft are monitored and recorded over the duration of the test. Critical details of the test such as temperature and vibration limits are undisclosed as these are considered propriety information.

## 4. REPAIRER EXPERIENCE REGARDING TIT

### *4.1 Rotor Failures and Failure Mechanisms in Practice*

An investigation was conducted to determine the frequency and impact with regards to TIT as experienced by a local repairer. Results from a total of 60 TITs performed on generator rotors over the period from 2007 to 2014 were investigated. These rotors are rated from 200MW to 900MW and age between 20 and 30 years old. Figure 1 summarises the test results per year. Of the 60 rotors tested during this period, 35 rotors passed and 25 rotors failed. This significantly high failure ratio of 42% indicates a need for further investigation into TIT methods.

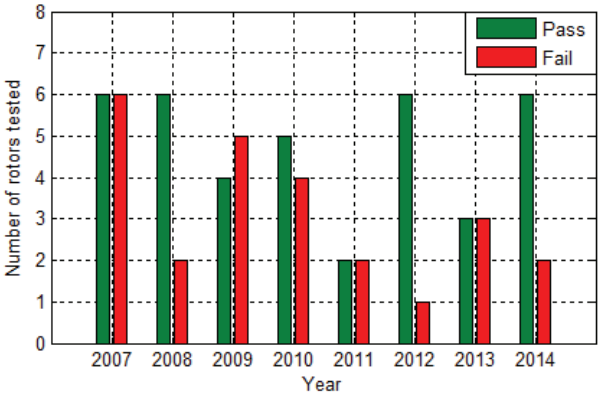


Figure 1: TIT results for 60 rotors, over an 8 year period, as experienced by repairer

Figure 2 was further analysed for the entire period to identify the most prevalent mechanisms of failure. Thermal sensitivity constituted the majority of failures at 88% while inter-turn shorts made up 8% followed by earth faults with 4%. Most rotors failed due to a combination of coil movement, non-uniform windings, blocking, body wedges and tight slots. The thermal sensitivity failure mechanism is used to represent this category of failure mechanisms due to the uncertainty in distinguishing between them. An earth fault is not identified as one of the significant mechanisms but was experienced. Analysis of the data indicates an increase in thermal stability failures which severely affects generating capacity and prolongs the return to service of generating units. This brings about the question if the testing methodology used for the past 20 years is still

valid or effective. Global TIT trends and practices need to be further investigated in order to improve or validate the currently accepted methodology.

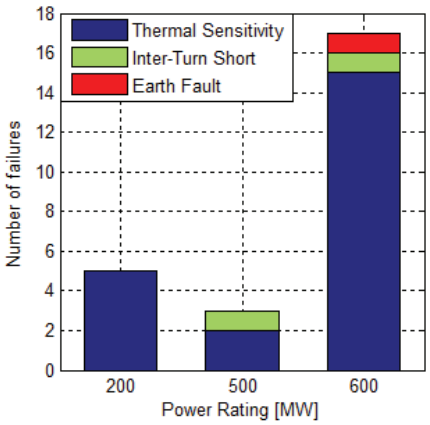


Figure 2: Prevalent mechanisms of generator failure as experienced by repairer

*4.2 TIT Methodologies in Practice*

Locally, testing is typically performed in a specialized 300-ton balancing facility which is designed to accommodate brushless as well as brushed rotors. Different sizes of Faraday Cages are also used depending on the rotor length. In brief, a test is conducted by exciting the rotor at different current levels starting at 400 A and - depending on the rotor design - ending at 1500 A. A soaking period is observed for every increment in current excitation. The vibration (magnitude and phase) and temperature are recorded at five minute intervals. A rotor that exhibits vibration levels outside prescribed design limits fails the thermal instability test and is deemed unsuitable for service [5]. Preliminary data gathered regarding global TIT preferences is displayed in Figure 3 [6 - 15]. The data was gathered from consultations with various OEM and non-OEM service providers. Analysis of these data indicates that different balancing facilities around the world prefer to use different methods for TIT owing to propriety reasons. Additionally, there is an even distribution between the two aforementioned methods of TIT. The lack of a specific preference globally also indicates that a more detailed investigation into which method is better suited to determining rotor thermal instability is required.

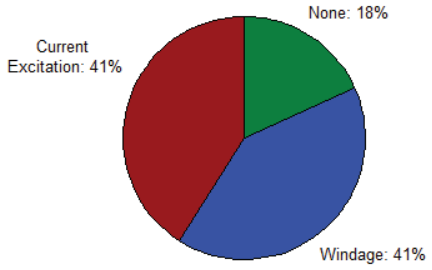


Figure 3: Summary of TIT preferences of 22 different testing facilities (data sourced from [6 - 15])

## 5. THERMAL ANALYSIS OF GENERATOR ROTORS UNDERGOING TIT

The generator rotor is a highly stressed component as it is subjected to centrifugal forces, torsional stresses and high cycle fatigue. The rotor is composed of a number of different materials such as copper, various insulation materials, steel, aluminium etc. The properties of these materials may vary drastically from each other in material strength; coefficient's of friction; coefficients of expansion and thermal conductivity, just to name a few. These unique compositions of materials and properties have to interact harmoniously for the rotor to perform its primary function within the design limits [16]. Taking into account the distinctive design of the generator rotor a thermal analysis of its behaviour may be conducted analytically using lumped-circuit models or via numerical methods such as finite-element analysis (FEA) and computational fluid dynamics (CFD). The suitability of these techniques need to be determined/considered [17].

Lumped parameters or thermal resistance networks can be used to model the heat transfer within the generator rotor in the form of a simplified characterisation. The approach involves calculating the conduction, convection and radiation resistances of different parts of the rotor and modelling these parameters in terms of an electrical circuit equivalent for thermal analysis. This method of thermal analysis is better suited to approximate design applications and does not have the level of detail required to analyse the specific issues of TIT [18].

FEA and CFD can be used to model complex geometries and include detailed material properties. These methods are demanding in terms of computational power and complexity. Successful discretisation of the generator rotor model will therefore require simplification resulting in loss of critical details. The simulation will lose accuracy as a result and the solution may not be indicative of the true thermal performance of the rotor [19 - 22].

All of the above methods may be well suited to the design evaluation of the thermal performance of a generator rotor. However, the difficulty arises when specific tolerances and assembly differences arise during the repair or rewind process of the rotor that cannot be accounted for by the model. Years of operation and maintenance alters the rotor components and tolerances from the initial design specifications. Even if these parameters were could be determined, the resources required to perform simulations for every rotor design undergoing TIT would not be feasible. Hence, a practicable method is required to determine the thermal performance of the rotor that takes into account all the parameter variations arising from operation and rework.

During TIT, the winding temperature of the rotor may be also be determined using a numerical calculation. One of the following equations may be utilised [23]:

$$T_{HOT} = \left\{ \left( \frac{R_{HOT}}{R_{COLD}} \right) \left( 234.5 + T_{COLD} \right) \right\} - 234.5 \quad (1)$$

$$\Delta T = \frac{\left( \frac{R_T}{R_0} \right) - 1}{\alpha} \quad (2)$$

where $R_{HOT}$ is the winding resistance at the testing point, $R_{COLD}$ is the winding resistance at the reference temperature, $T_{COLD}$ is the reference temperature value, 234.5˚C is a standard temperature coefficient for copper, ΔT is the change in temperature, $R_T$ is the resistance at a specific temperature, $R_0$ is the resistance at zero degrees Celsius and $\alpha$ is the co-efficient of expansion for copper. From (1) and (2), it can be seen that the resistance as well as a physical temperature measurement must be known at a specific current and voltage level. Thereafter, the subsequent temperature rises can be calculated by utilising the rotor resistance measurement. The resistance measurement needs to be accurate and can be significantly affected by the slipring/brush gear interaction. On the other hand - when the friction method of TIT is preferred - current injection is still used as a method to determine winding resistance and calculate the temperature. This method excludes the temperature of the rotor body, wedges, pole faces, shaft, retaining rings and other extremities of the rotor assembly. The uneven thermal profiles of all of these components can lead to thermal instability. The presented direct mapping method can pin-point areas of concern and reduce guess-work during trouble shooting. It physically determines and maps the winding and body temperature of the rotor which eliminates the uncertainties posed by contemporary testing methodologies.

## 6. DIRECT MAPPING METHODODLOGY

### *6.1 Infrared (IR) Sensors*

The widespread use of infrared thermography within the electrical industry has become commonplace for a number of years [24, 25]. This non-contact method produces reliable and accurate results for fault finding and trouble shooting. Temperature measurements are made possible by detecting the radiant flux of an object and through a calibration algorithm a temperature output is calculated. Also referred to as a radiation thermometer many varieties are available on the market today, from thermal imaging cameras to singular probes. Devices are able to measure a wide variety of temperature ranges and can operate at high speeds making it ideal for the proposed test setup [26].

### *6.2 Temperature Map*

The preferred method for data capture is in the form of a matrix of temperature values corresponding to the spatial mapping of the surface of the generator rotor. The presented method transforms these temperature measurements and physical coordinates into a 2-D thermal map. Simply put, the direct thermal mapping method presents the 3-D data (temperature and surface area of the rotor) as a 2-D colour map (commonly referred to as a heat map). The map consists of a number of rectangular rows and columns that represent data values against a colour scale. This method has been widely used to display large matrices within many different fields such as natural and biological sciences [27, 28]. Ultimately, the experimental setup is required to map the temperature distribution of the rotor and output data that can lead to the information being displayed as a thermal map for easy interpretation and instability detection. Each block within the thermal map represents a measurement pixel of the IR camera and each pixel of the IR camera represents a physical portion of the rotor. The distance of the IR camera from the rotor determines the physical size of the area that is sampled.

### *6.3 Experimental Setup*

The experimental test setup uses a mini-rotor rated at 20 kVA that is designed to mimic a 600 MW generator rotor. Table 1 summarises the constructional details of both the mini-rotor and a typical 600 MW generator rotor. The rotor is similar to a 600 MW rotor in the following aspects:

- Two-pole 3000 rpm, 50 Hz
- Distributed and concentric field windings
- Damper bars
- Shaft mounted slip rings
- Insulated bearings
- Mono-block milled shaft with slots

Table 1: Comparison of specifications of Mini-gen and turbine-generator rotors

| Parameter | Mini-rotor | 600 MW |
|---|---|---|
| Rotor slots | 32 | 32 |
| Damper bars | 48 | 48 |
| Rotor diameter | 178.5 mm | 1165 mm |
| Shaft length (journal centres) | 885 mm | 10990 mm |
| Shaft diameter | 67 mm | 530 mm |

A 3-D model of the constructed test setup is shown in Figure 4. The rotor is driven by an induction motor rated at 3000 rpm. The enclosure of the setup is also scaled to simulate a local balancing facility. The scaling is based on the length of the rotors thus the mini-rotor is down-scaled approximately to the ratio 2:25 when compared to a conventional 600 MW rotor. The enclosure was designed around this scaling factor when compared to the balancing facility's dimensions. It was constructed using 12 mm fibre board and insulated with a number of layers of styrofoam to mimic the insulative and dimensional properties of the full-scale balancing facility. The test

setup utilises a high speed high resolution 80 Hz IR Camera (2% error margin) that captures the surface data of the rotor through a viewing window. This is achieved by defining an array of pixels that only sample the area of the rotor directly below to camera. The pixel width and length is calculated according to the rotor surface area and IR Camera sample rate to enable a full mapping of the rotor surface. The rotor body is painted black to improve accuracy of the data captured as IR technology responds better to black bodies translating to a higher emissivity [26]. The winding temperature is captured with a laser guided IR pyrometer with the copper windings also painted black to improve accuracy. A proximity probe is used to differentiate each revolution of the mini-rotor. This is achieved with the aid of a fixed collar with a machined notch. The output is received when the notch passes the proximity probe and indicates when one revolution has passed. A number of thermocouples are also used to monitor the ambient temperature as well as the temperature within the enclosure. Thermocouples are positioned on either side of the mini-rotor with pairs of thermocouples near the slipring, the centre of the body as well as near the drive end. During the temperature mapping process, the rotor speed was decreased via controlling the speed of prime mover (induction machine). Rotational speed was reduced to 60 rpm with consideration of the maximum sampling rate of the camera. Upon completion of the mapping process, the rotor speed was ramped back to 3000 rpm. A number of test conditions are investigated to prove that the setup is viable for intended purpose.

## 7. EXPERIMENTAL TESTING AND RESULTS

### *7.1 Test Condition 1 – No Excitation Including Brush Gear*

The initial investigation entails mapping of the mini-rotor without excitation conditions using the previously described experimental setup.

This test involves heating the rotor by air friction or windage while the brush gear remains connected. The test runs for eight hours and readings are taken at 30 min intervals. Figure 5 shows the results obtained after 480 minutes. Figure 6 shows the average temperature distribution along the axial length of the rotor corresponding to the thermal map given in Figure 5. The difference in the average temperature of the drive and non-drive ends of the rotor varies up to 4 °C during the testing procedure. This is a significant observation as relatively small differences in temperature can lead to thermal sensitivity. This could be attributed to either bearing losses, rubbing at the non-drive end or the frictional interaction of the slip-ring and brush gear. The test was repeated after disassembling the brush gear to confirm the source of the temperature gradient.

### *7.2 Test Condition 2 – No Excitation Excluding Brush Gear*

The second test condition is carried out with the brush gear disassembled thereby allowing the rotor to move freely on the pedestal bearings. This test follows the same methodology as previously described in Test Condition 1. The thermal map resulting after 480 minutes – without excitation and excluding the brush gear – is given in Figure 7. The corresponding average temperature distribution, along the axial length of the rotor, is shown in Figure 8.

### *7.3 Test Condition 3 – With Excitation*

For this test condition, the rotor is operated at 3000 rpm with different levels of excitation - i.e. 5 A, 10 A, 20 A and 35 A. Each excitation level is sustained for an hour with measurement taken at 10 min intervals. Figure 9 illustrates the thermal map obtained at 35 A, after 10 minutes. The corresponding average temperature distribution, along the radial circumference of the rotor, is shown in Figure 10.

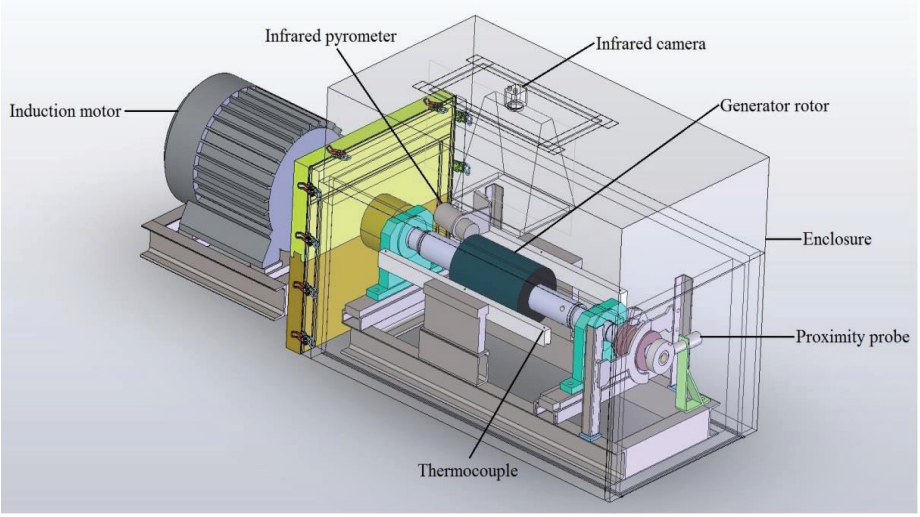


Figure 4: Experimental configuration used for rotor thermal instability testing and measurement.

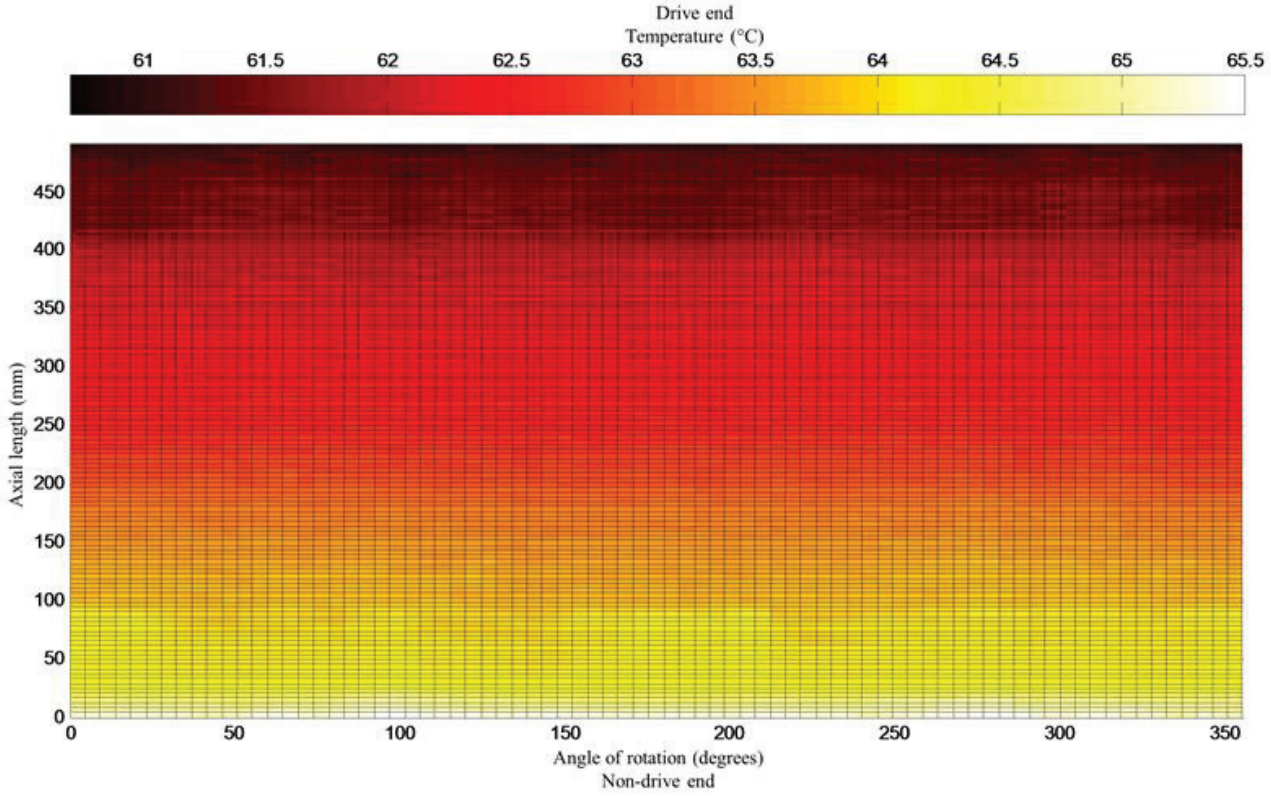


Figure 5: Thermal map of rotor for test-condition 1 i.e. no excitation including brush gear after 480 min

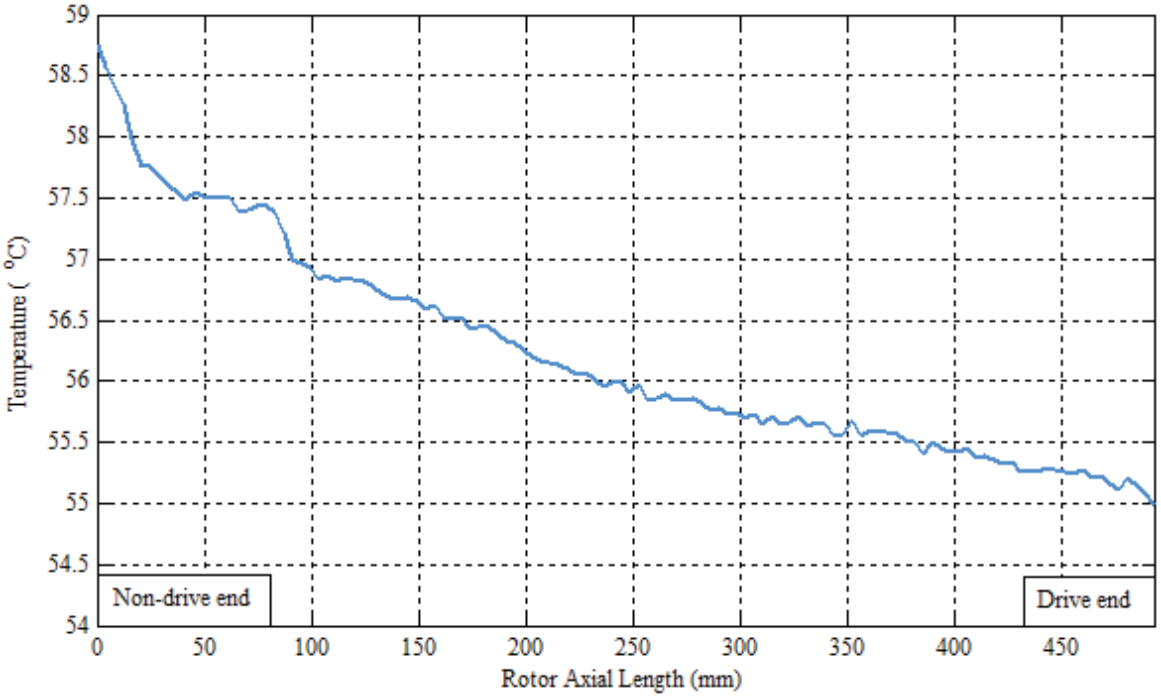


Figure 6: Average temperature distribution along axial length (no excitation including brush gear after 480 min)

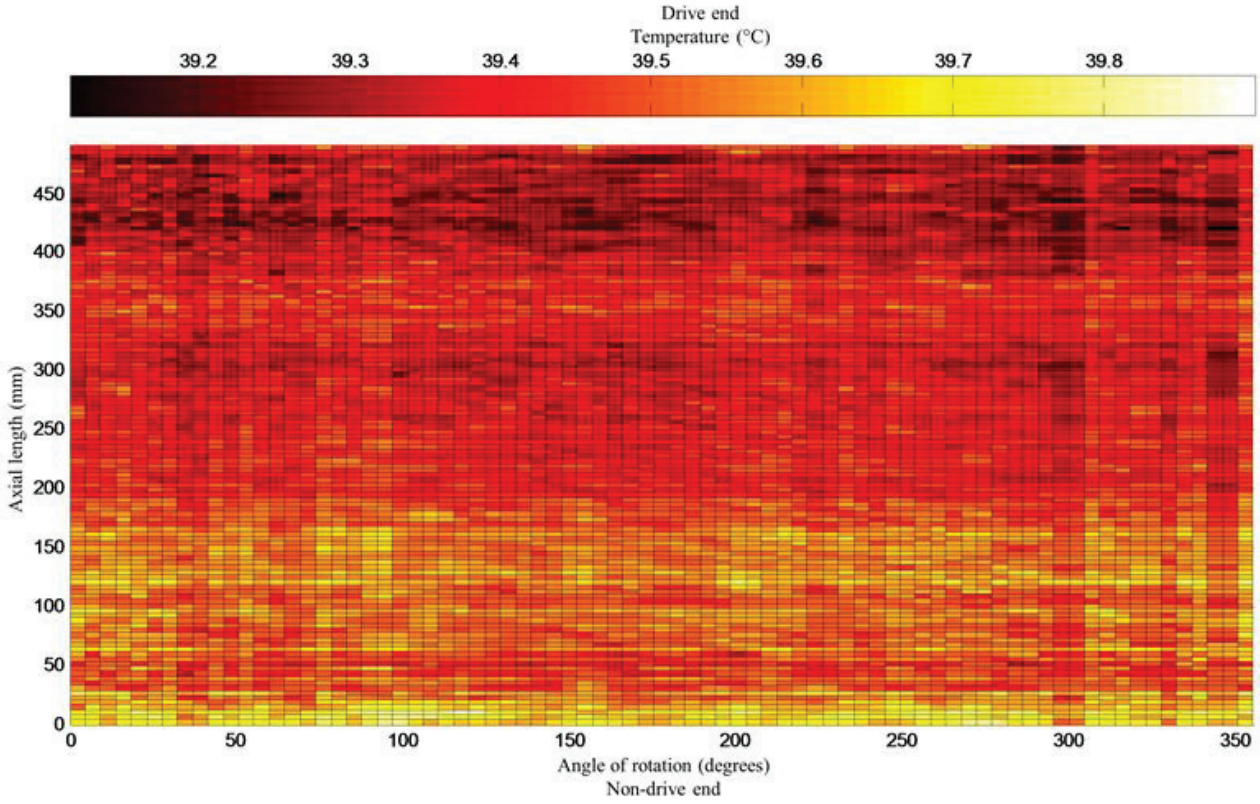


Figure 7: Thermal map of rotor for test-condition 2 i.e. no excitation excluding brush gear after 480 min

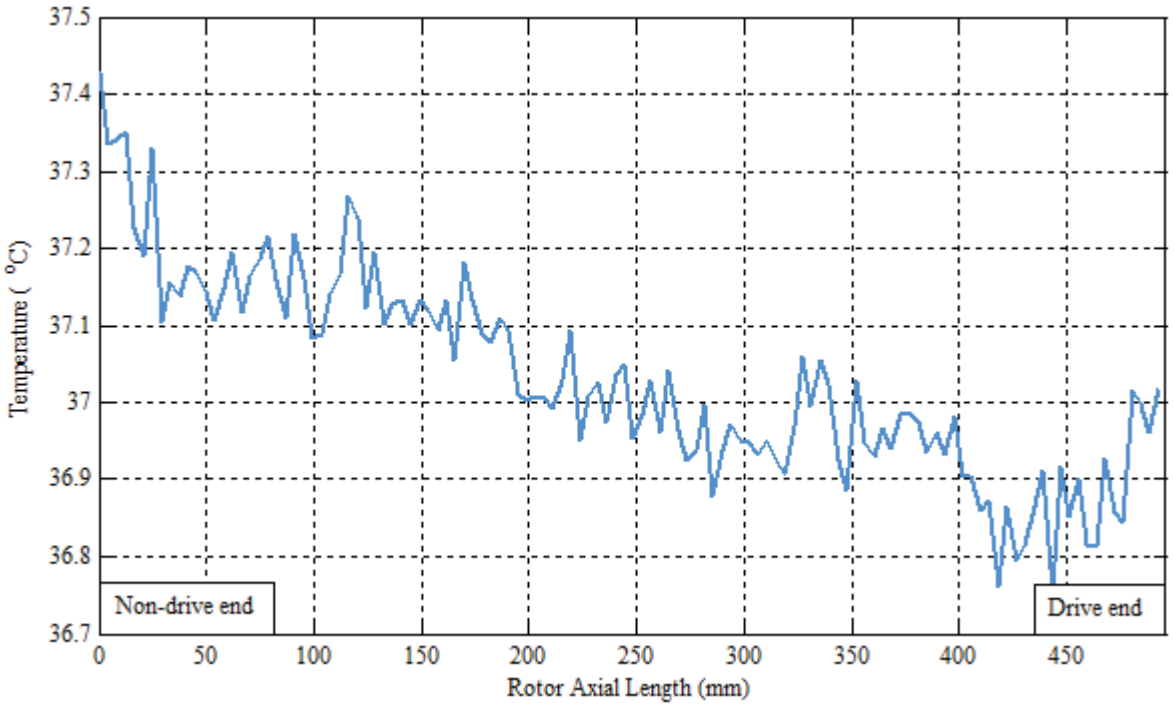


Figure 8: Average temperature distribution along axial length (no excitation excluding brush gear after 480 min)

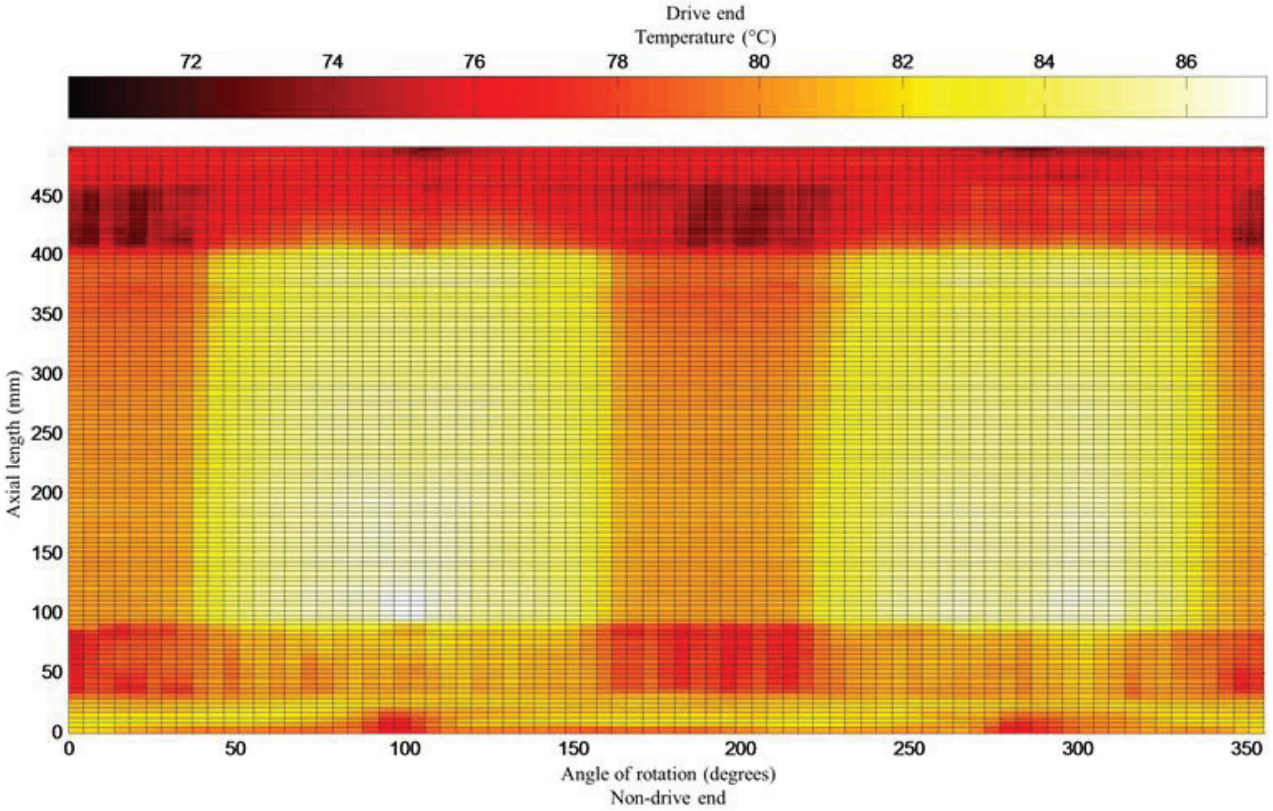


Figure 9: Thermal map of rotor for test-condition 3 i.e. with 35 A current excitation after 210 min

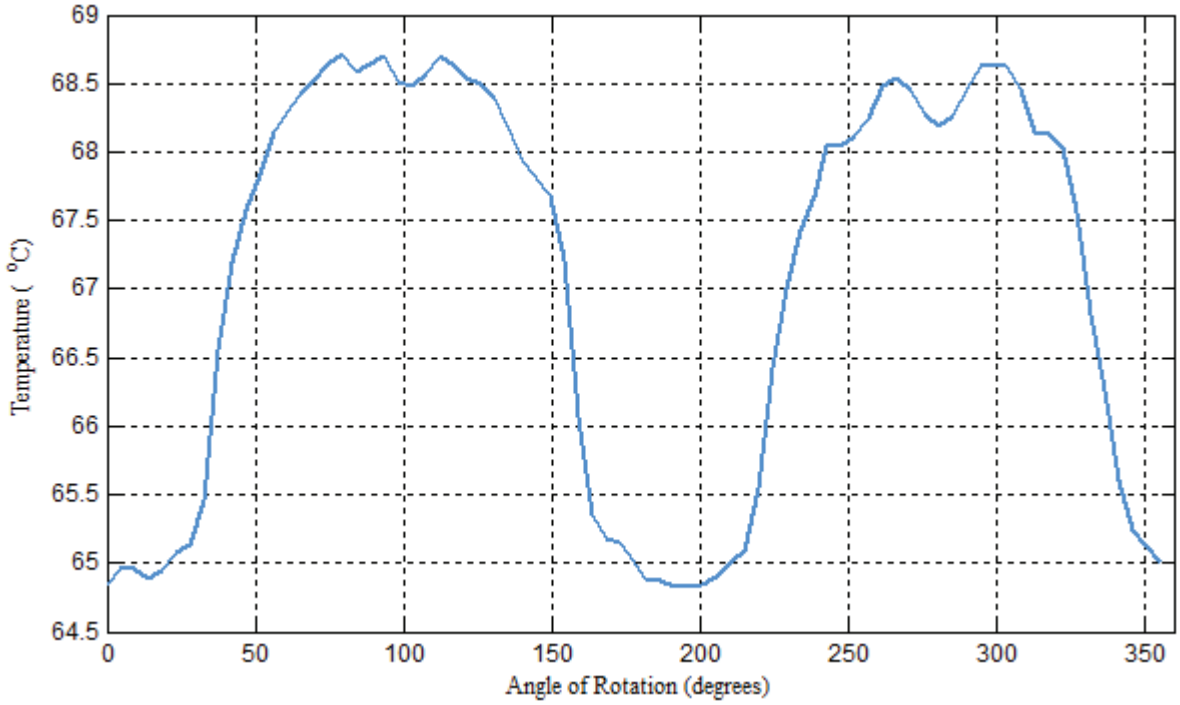


Figure 10: Average vertical temperature distribution along circumference at 35 A, 210 min

*7.4 Test Condition 4 – Inter-turn Short-Circuit Fault*

The final test condition is carried out with the aim of verifying the capability of the presented method to detect and locate a fault or abnormality on the rotor body e.g. locating the slot where an anomaly is occurring resulting in uneven heating. This will determine if the direct thermal mapping method can be an effective fault finding tool once a thermal sensitivity problem is experienced and may assist in avoiding unnecessary expenses related to large turbo-generator rotor fault finding and disassembly. During this test condition, an inter-turn short is induced between turns six and seven on coil eight of a pole as illustrated in Figure 11 of the mini-rotor and excitation applied at 20 A. The rotor is then thermally mapped after 30 s.

*7.5 Discussion*

The thermal maps have a suitably high resolution of 120x77 points. Each point measured is represented by a 4.14 mm x 6.9 mm section of the rotor body. The presented test method enables 94 % of the total surface of the rotor body to be mapped. Figures 5, 7 and 9 show considerable differences in the rotor thermal signatures under the different test conditions. Test condition 1 showed significant detail with respect to the heating of the winding and the transmission of the heat to other parts of the rotor. The average surface temperature is found to be 67°C while the winding temperature is 67.1°C.The thermal map for test condition 2 shows relatively uniform heating of the rotor body. There is also a distinct thermal gradient along the axial length of rotor where the slip-ring end of the rotor experienced a higher temperature as compared to that of the drive end. The average body temperature is measured to be 56.2°C with a winding temperature of 47.3°C – i.e. a difference of 8.9°C. Thus the measurement of the winding temperature alone does not yield a true indication of the surface temperature of the rotor body. The results obtained from test condition 3 indicate that the interaction between the brush gear/slip-ring assembly and shaft significantly contributes to the heating of the rotor. The friction created between these components alone is capable of heating the rotor in test-condition 1 to a significantly higher temperature. The average temperature of the rotor body is 37°C and the winding is measured 33°C. Furthermore, this scenario also yielded a substantial difference between the winding and body temperatures - i.e. 4°C.

This evaluation illustrates that FTIT has a relatively slower rate of heating that begins at the surface of the rotor. It should be noted that FTIT can be affected by the slip-ring brush-gear interaction leading to a skewed thermal distribution that is not indicative of the rotor's true thermal performance under friction as illustrated when the brush-gear was removed. It was expected that frictional heating would be a gradual process resulting in even heating of the rotor. However, the significant influence of the brush-gear was not expected. The current injection that characterises CTIT resulted in the winding being the main heat source. The heat then radiated to other parts of the rotor body. The temperature distribution was not symmetrical, even though the rotor also experienced the effects of frictional heating. The windings of the poles were clearly visible. The clear mapping of the winding area and pole faces was unexpected but the rapid heating and higher surface temperatures experienced during CTIT were anticipated.

In test condition 4, the problem area was located approximately 100 degrees about the angle of rotation - at the non-drive end - of the mini-rotor. This location was physically verified on the mini-rotor and corresponds to the location of the induced inter-turn short. Furthermore, the fault condition was detected within 30 seconds of current injection.

## 8. CONCLUSION

A methodology for directly mapping the thermal distribution of an experimental generator's rotor was presented in this paper. An experimental setup was developed and constructed to scale in order to map the surface of a mini-generator rotor. In addition to the direct mapping of the surface temperature, this configuration is equipped to directly measure the winding temperature and other key temperature points within the experimental enclosure. Results indicate significant dissimilarities between the different methods of TIT contrary to the non-preferential TIT practices in industry. This emphasizes the need to modernize current TIT practice with methods such as the presented thermal mapping method. In summary, the mini-rotor responded differently during the three test conditions – i.e. without current excitation (including and excluding brush gear) and with current excitation. Testing of the direct mapping method for the additional fault scenario of an inter-turn short-circuited winding yielded fast and accurate results with regards to detection and localization. Ultimately, the direct-mapping method produces a detailed representation of the thermal behaviour of the rotor and provides the potential to not only further understand the shortcomings of TIT but to assist with augmentation thereof.

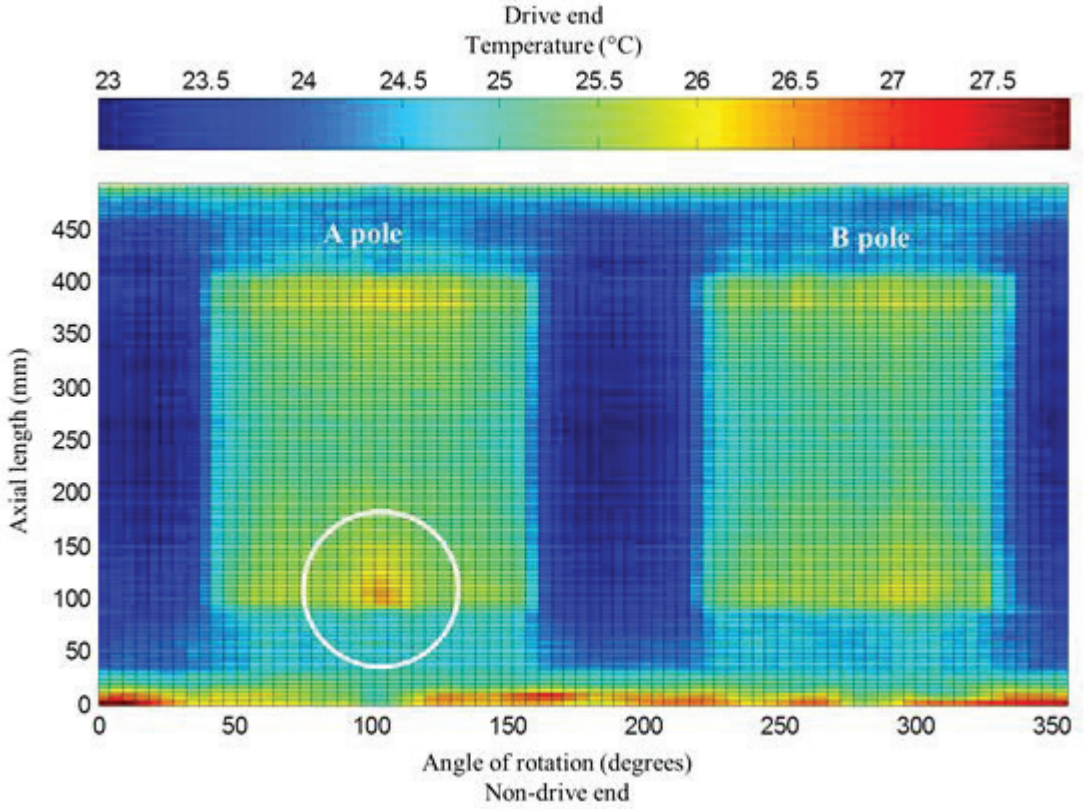


Figure 11: Thermal map of rotor for test-condition 4 – i.e. inter-turn short-circuit fault.

## 9. REFERENCES

[1] G. Klempner and I. Kerszenbaum: "Operation and Maintenance of Large Turbo-Generators", Power Engineering, John Wiley & Sons, 2004

[2] M. Jevtić, V. Zeljković and M. Dapić: "Thermal influences on turbogenerator dynamic behaviour", Elektrotechnika i Elektronika, Vol. 25, pp. 157-161, 2006.

[3] G.A. Juhlin: "Deformation of Turbo-Alternator Rotor Windings, Due to Temperature Rise", *Journal of the Instituite of Electrical Engineers*, Vol 85, pp. 544-522, 1939.

[4] R.J. Zawaoysky, and W.M. Genovese: "Generator Rotor Thermal Sensitivity – Theory and Experience", GE Reference Library, GER-3809,2001

[5] B. Irwanto, L. Eckert and T. Prothmann: "Thermal Unbalance Behaviour of Turbogenerator Rotors", 9th IFToMM International Conference on Rotor Dynamics, Springer, 2015.

[6] Turbo Gen Services: "High Speed Balancing Specifications for Generators", Eskom South Africa, TWG-F-23, 2013.

[7] J. Cockerille: "Private communication", May 2015.

[8] G. Csaba: " Private communication", May 2015.

[9] B. Moore: " Private communication", May 2015.

[10] M. Ohm: "Private communication", May 2015.

[11] S. Plessie: " Private communication", May 2015.

[12] D. Rennie: " Private communication", May 2015.

[13] A. Thackray: "Private communication", August 2015.

[14] D.J. Pierre: "Private communication, September 2015.

[15] S. Robinson: "Private communication", June 2015.

[16] G.C. Stone, I. Culbert and H. Dhirani: "Electrical Insulation for Rotating Machines", Power Engineering, John Wiley & Sons, 2004.

[17] A. Boglietti, A Cavagnino, D. Staton, M. Shanel, M. Mueller, and C. Mejuto: "Evolution and modern approaches for thermal analysis of electrical machines", IEEE Transactions on Industrial Electronics, Vol 56, pp. 871-882, 2009.

[18] J. Nerg, M. Rilla, and J. Pyrhonen: "Thermal analysis of radial-flux electrical machines with a high power density", IEEE Transactions on Industrial Electronics, Vol 55, pp. 3543-3554, 2008.

[19] A. Boglietti, A. Cavagnino and D. Staton: "Determination of critical parameters in electrical machine thermal models", *IEEE Transactions on Industry Applications*, Vol 44, pp. 1150-1159, 2008.

[20] D. Dorrell, D. Staton, and M. McGlip: "A combined electromagnetic and thermal approach to the design of electrical machines", Proc. Int. Conf. Elect. Mach. Syst., 2006.

[21] C. Mejuto, M. Mueller, M. Shanel, A. Mebarki, M. Reekie, and D. Staton: "Improved synchronous machine thermal modelling", 18th International Conference on Electrical Machines, IEEE, 2008.

[22] M. Mohammadi, H. Ansari, P. Bahemmat, and A.A. Kharamani: "Thermal analysis of the rotor of large air-cooled turbo generators", Proceedings of the 3rd Conference on Thermal Power Plants (CTPP), IEEE, 2011.

[23] A. Boglietti, E. Carpaneto, M. Cossale, S. Vaschetto, M. Popescu, and D. A. Staton: "Stator winding thermal conductivity evaluation: An industrial production assessment", IEEE Transactions on Industrial Applications, Vol 52, pp. 3893-3900, 2016.

[24] A.J. Holliday and J. Kay: "The use of infrared viewing systems in electrical control equipment", Conference Record of 2005 Annual Pulp and Paper Industry Technical Conference, IEEE, 2005.

[25] T Suesut, N. Nunak, T. Nunak, A. Rotrugsa, and Y. Tuppadung: "Emissivity measurements on material and equipment in electrical distribution system", 11th International Conference on Control, Automation and Systems (ICCAS). IEEE, 2011.

[26] D.P. DeWitt, and G.D. Nutter: "Theory and practice of radiation thermometry", Wiley Online Library, 1998.

[27] C.H. Chen: "Generalized association plots: Information visualization via iteratively generated correlation matrices", Statistica Sinica, Vol 12, pp. 7-30, 2002.

[28] L. Wilkinson, and M. Friendly: "The history of the cluster heat map", The American Statistician, Vol 63, 2009.